Conference Paper, Published Version

Ferreira da Silva, Ana Maria; Ahmari, Habib

Internal Structure of an Alternate Bar Inducing Flow

INTERNAL STRUCTURE OF AN ALTERNATE BAR INDUCING FLOW

Ana Maria Ferreira da Silva[1] and Habib Ahmari[2]

[1] Professor, Department of Civil Engineering, Queen's University
Kingston, Ontario, Canada K7L 3N6, e-mail: amsilva@civil.queensu.ca
[2] Ph.D. Candidate, Department of Civil Engineering, Queen's University
Kingston, Ontario, Canada K7L 3N6, e-mail: ahmari@ce.queensu.ca

ABSTRACT

In this paper, the size of the largest horizontal coherent structures (HCS's) of turbulence in open-channel flows is investigated; and the dynamics and alluvial consequences of these structures are explored. The analysis is carried out on the basis of three series of flow velocity measurements in a 21m-long, 1m-wide and 0.40m-deep channel. The horizontal burst-length was found to be between four and seven times the flow width; an internal meandering of the flow caused by the superimposition of burst-sequences on the mean flow was detectable. Both of these findings support the view that alternate bars are the "imprints" on the mobile bed of HCS's.

Keywords: Horizontal coherent structures, burst length, dynamics and alluvial consequences

1. INTRODUCTION

Alternate bars are large-scale bed forms, characterized by gentle upstream slopes and deep pools at the beginning of their diagonal crests, implying a pattern of alternating holes along the side walls or banks (see Figure 1). These bed forms occur in relatively shallow flows having, according to da Silva (1991), Yalin and da Silva (2001), values of the width-to-depth ratio B/h falling between those of lines $\mathcal{L}$ and $\mathcal{L}_A$ in Figure 2 (where h/D is the flow depth h relative to the grain size D of the cohesionless alluvium). The length of alternate bars scales with the flow width (their average length is approximately six times the flow width B (Hayashi 1971; JSCE 1973; Yalin 1992, etc.)).

It is known since a long time that no periodic (along the flow direction x) bed forms can be produced by a laminar flow (see e.g. Tison 1949). This led many earlier prominent researchers dealing with dunes to attribute the occurrence of these bed forms to the large-scale turbulence, and in particular to view dunes as a "manifestation" of the structure of turbulence in the vertical planes of the flow. This view eventually gave rise to the idea that the reason for the occurrence of alternate bars lies also in the structure of large-scale turbulence. Kishi (1980) and Jaeggi (1984) appear to have been the first to hint at this possibility, and to suggest that alternate bars are but the "horizontal version" of dunes. Indeed, the fact that alternate bars scale with the flow width B whereas dunes scale with the flow depth h, as well as the striking similarity between the expressions of dune length ($\Lambda_d \approx 6h$) and alternate bar length ($\Lambda_a \approx 6B$), strongly suggest the existence of a mechanism in the horizontal planes of the flow responsible for the occurrence of alternate bars, analogous to the turbulence mechanism inherent in the vertical planes of the flow and ultimately responsible for the occurrence of dunes. This idea is further strengthened by similarities also in the process of formation of sequences of dunes and sequences of alternate bars. These include, among others, the fact that the development of these two types of bed forms, as evidenced by numerous laboratory experiments, is an "activity" that starts from a section $x = 0$ (usually the beginning of the mobile bed) and propagates downstream.

Figure 1. Alternate bars in a laboratory flume (from da Silva 1991)

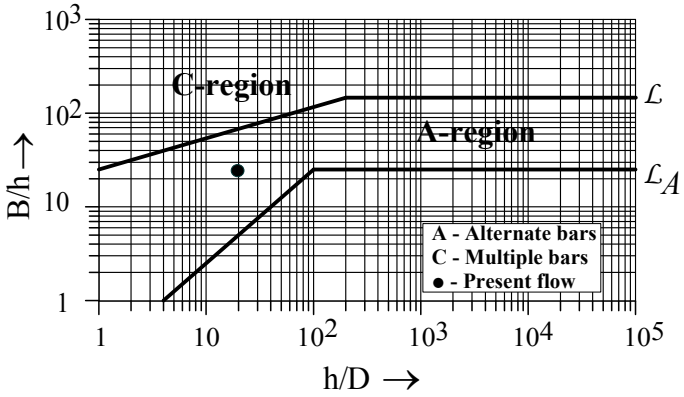

Figure 2. The $(B/h; h/D)$ -plan defining the existence region of alternate bars (after da Silva 1991 and Yalin and da Silva 2001)

However, it was only after the relatively recent discovery of bursting processes and coherent structures by turbulence researchers that it became possible to properly link the occurrence of dunes and alternate bars to turbulence. Following Hussain (1983), a "coherent structure" is defined in this paper as the largest conglomeration of turbulent eddies which has a prevailing sense of rotation, the term burst designating the evolution of a coherent structure during its life-span *T*. The bursts can be vertical or horizontal. The coherent structures of the former rotate in the vertical $(x;z)$ -planes, those of the latter in the horizontal $(x;y)$ -planes, vertical and horizontal structures co-existing in the same flow.

As can be inferred from the reviews on the topic by e.g. Nezu and Nakagawa (1993) and Roy et al. (2004), vertical coherent structures in a variety of flows, including open-channel flows, have since the mid 70's been the object of a very large number of studies. On the basis of these studies, Yalin (1992) has convincingly explained the occurrence of dunes as the "imprints" on the mobile bed of periodic sequences of vertical bursts. In particular, this author dealt in detail with the "imprint mechanism", and showed that several features of the dune development process can be comprehensively explained on the basis of vertical coherent structures.

By considering earlier river and open-channel flow measurements and observations (such as those by Yokosi 1967, Dementiev 1962 and Grishanin 1979) in the light of the present understanding on coherent structures, together with the available field and laboratory data on alternate bar geometry, da Silva (1991), Yalin (1992) and Yalin and da Silva (2001) concluded that alternate bars are most likely the "imprints" on the deformable alluvium of horizontal coherent structures. Yet, in contrast to the case of vertical turbulence and dune-inducing flows, no systematic studies focusing specifically on horizontal turbulence and/or on the internal structure of flows capable of producing alternate bars have been carried out to date. As a result, the existing evidence linking horizontal coherent structures and alternate bars remains very limited. Thus, the explanations regarding the formation of alternate bars by the just mentioned authors, in their detail, rely to a large extent on generalizations of aspects of the life-cycle of vertical coherent structures to the case of horizontal coherent structures, and on deductions regarding the nature of the horizontal turbulence structures based on the nature of their "imprints" (alternate bars). Considering this, and in order to address the lack of pertinent data on the topic, the authors have initiated an extensive experimental study of the nature of an alternate bar inducing flow. The objective of this paper is to report the first measurements of this study and present their preliminary results. It is hoped that this and similar studies will lead to a better understanding of the internal structure of alternate bar inducing flows, as well as the process of formation of alternate bars.

2. COHERENT STRUCTURES AND BURSTING PROCESSES: FUNDAMENTALS

Before proceeding further, the following pertinent aspects of coherent structures and bursts should be mentioned.

i) Although many details of how exactly coherent structures originate and develop are not yet known, the life-cycle of vertical coherent structures can, on the basis of Blackwelder (1978), Cantwell (1981), Gad-el-Hak and Hussain (1986), Hussain (1983), Rashidi and Banerjee (1988) and several others, very briefly be synthesized as illustrated in the conceptual Figure 3a (showing, in a stationary frame, a vertical burst-cycle of an open-channel flow). A vertical coherent structure originates around a point *P*, at a location O_i, with the rolling-up at time $t = 0$, say, of a future macroturbulent eddy e_V. This is then ejected away from the bed, together with the fluid around it, and continues to move away from the bed while it is transported by the flow downstream: thus a continually growing coherent structure comes into being. When this structure becomes as large as to touch the free surface, it disintegrates (break-up phase) into a multitude of smaller and then even smaller eddies, until they become as small as the lower limit ν / v_*, where their energy is dissipated. The "break-up" of a coherent structure prompts the birth of another at O_{i+1}. The distance $O_i O_{i+1}$ between the "birth-places" of two consecutive bursts of a vertical burst-sequence is the burst length λ_V, the life-span of a burst (i.e. the burst period) being $T_V = \lambda_V / v$, where v is the average flow velocity (for the coherent structures are transported by the flow with the velocity $\approx v$). The vertical burst-length is known to scale with the flow depth, i.e $\lambda_V \approx \alpha h$, where α is a coefficient of proportionality (Jackson 1976; Yalin 1992; Roy et al. 2004).

The cine-record in Figure 3b shows (in a convective frame) an instantaneous view of two consecutive vertical coherent structures.

ii) The related observations and measurements indicate that horizontal turbulence too has its coherent structures and bursts. Although as mentioned earlier, horizontal coherent structures have not yet been the focus of directed research, there are reasons to believe that in their life-cycle they follow, *mutatis mutandi*, the events described above in paragraph (i), but with these

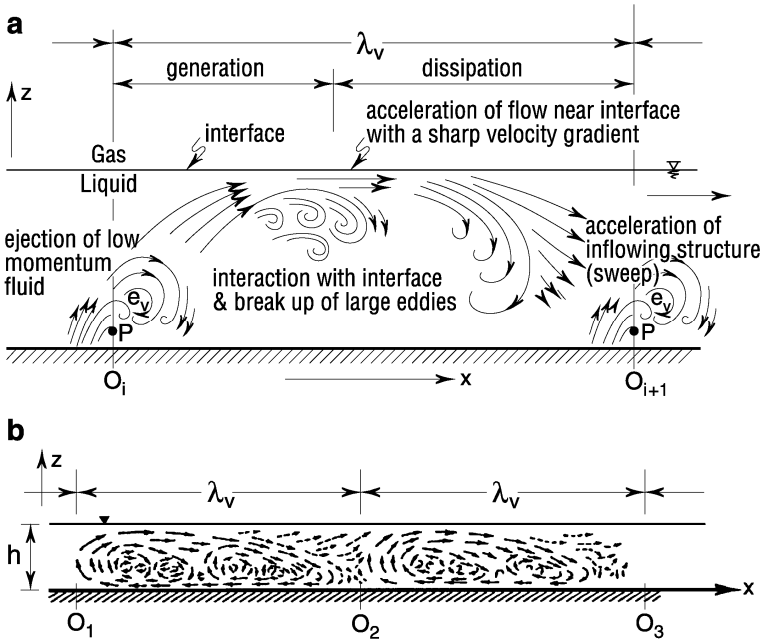

Figure 3. (a) Schematic representation of a vertical burst-cycle in an open-channel flow; (b) Cine-record showing an instantaneous view of two consecutive vertical coherent structures (from Klaven 1966).

occurring in a horizontal "flow ribbon". This means that h, λ_V, T_V, ... in (i) are to be replaced by B, λ_H, T_H, etc. The horizontal coherent structures (henceforth referred to as HCS's) are likely to originate at the "points" P near the banks and the free surface, where horizontal shear stresses τ_{xy} are the largest, and from there be conveyed by the mean flow away from the bank and downstream while growing in size (see Figure 4). Once their lateral extent becomes as large as B, they must be expected to interact with the opposite bank and disintegrate, the neutralized fluid mass returning to its original bank so as to arrive there at $t = T_H$ (the burst length in this case being $\lambda_H = \alpha B$). There seems to be agreement that the coherent structures forming the horizontal bursts of a wide open-channel have the shape of horizontally positioned disks, eventually extending (along *z*) throughout the flow thickness *h* (see e.g. Grishanin 1979, Jirka and Uijttewaal 2004, Yalin 2006).

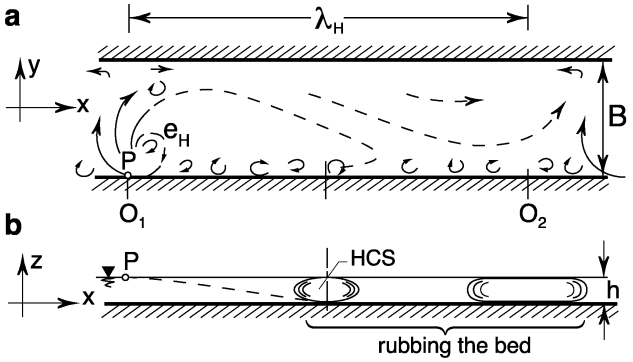

Figure 4. Schematic representation of a horizontal burst-cycle in an open-channel flow

iii) Bursts (vertical or horizontal) are randomly distributed in space and time. This implies that under completely uniform conditions of flow, there is an equal probability (or frequency) of occurrence of bursts for any region Δx and time interval Δt. As pointed out by Yalin (1992), such a homogeneous, or uniform, distribution of bursts along the flow direction x cannot lead to a wave-like deformation of the bed surface. According to this author, there must thus be in the flow a "location of preference" leading to the increment of the frequency of bursts at that location – and, since the break-up of one coherent structure (CS) triggers the "birth" of the next CS, leading also to the more frequent generation of sequences of bursts initiating from it, and eventually to the periodic deformation of the bed surface. In practice, this is realized by means of a local discontinuity (the section containing it thus becoming the preferential section, $x = 0$ say). In the case of laboratory conditions, the discontinuity can be the beginning of mobile bed or banks, an accidental ridge on the sand surface, etc.

The periodic deformation of the bed by the sequences of HCS's will be explored later, in view of the results of the present measurements.

3. EXPERIMENTAL SET-UP AND SPECIFICATION OF MEASUREMENTS

The present flow velocity measurements were carried out in a 1m-wide, 21m-long and 0.4m-deep straight channel (see Figure 5). The side walls of the channel were vertical and made of aluminium. The channel was installed in the 21m-long, 7m-wide river basin of the Civil Engineering Department at Queen's University. The basin is equipped with a water re-circulation system, the complete details of which are given elsewhere (e.g. da Silva and El-Tahawy 2008). The upstream end of the river basin consists of a 1.85m-wide and 8.8m-long stilling tank, a 0.60m-tall wall separating the stilling tank from the river basin. The water entered the present experimental channel through a 1m-wide opening on this wall. The channel bed was formed by a well-sorted silica sand, with an average grain size D_{50} of

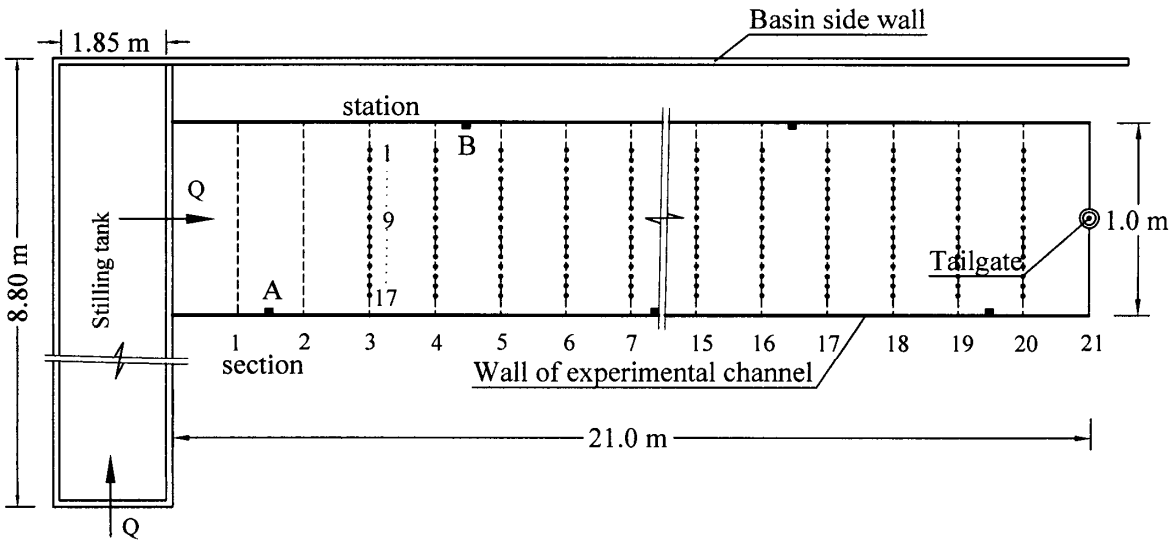

Figure 5. General view of experimental channel; location of flow measurements (stations 1 to 17 on cross-sections 3 to 20)

2mm, and a specific density of 2.65. To ensure that the bed material would not be removed from the bed at the entrance to the experimental channel, a 1m-long stretch of gravel of diameter ≈ 2.5 cm was installed at the upstream end of the channel. The surface of the sand bed was scraped so as to produce the desired stream slope, and a flat bed surface. The flow free surface slope was adjusted by means of a tailgate at the end of the channel.

The turbulent and sub-critical flow under investigation was uniform, with a flow depth of 4cm. The bed slope $S = 0.0015$ was selected so that, for the present flow depth, the bed shear stress acting on the bed would be substantially below the threshold for initiation of motion – thus ensuring that the bed would remain flat throughout the measurements. The hydraulic conditions of the flow are summarized in Table 1.

Table 1. Hydraulic conditions of the flow under investigation (B = 1m; D_{50} = 2mm)

Q (l/s)	h (cm)	S	v (cm/s)	Fr	Re	Re_*	Y/Y_{cr}	B/h	h/D
9.0	4.0	0.0015	22.5	0.36	9000	97	0.4	25	20

Here Q is flow rate, v is average flow velocity $(=Q/(Bh))$, Fr is the Froude number $(=v/\sqrt{gh})$, Re is the flow Reynolds number $(=vh/\nu$, where ν is the fluid kinematic viscosity), Re_* is the roughness Reynolds number $(=v_* k_S/\nu$, where $v_* = \sqrt{\tau_0/\rho} = \sqrt{gSh}$ is the shear velocity and k_S is the granular skin roughness ($k_S \approx 2D_{50}$; Kamphuis 1974)), and Y/Y_{cr} is the relative flow intensity ($Y = \tau_0/(\gamma_S D)$ being the mobility number and Y_{cr} the value of Y at the critical stage (stage of inception of sediment transport)). Here the symbols τ_0 and γ_S stand for bed shear stress and submerged specific weight, respectively. For the present sand, Y_{cr} was identified with 0.045.

Observe from the $(B/h; h/D)$-plan in Figure 2 that the present flow falls well in the midst of the alternate bar region. This indicates that the flow would indeed lead to the occurrence of alternate bars provided that the material on the bed would be able to move.

Three series of flow velocity measurements were carried out. Among these, the first series, termed MS-2B, is to be viewed as the main run. In this run, and in order to establish "locations of preference" for the generation of bursts and burst-sequences on both walls, two

10cm-long blocks with $2\text{cm} \times 2\text{cm}$ square bases (blocks A and B) were attached to the walls, with their longest side standing vertically and their square bases lying $\approx 2\text{cm}$ from the bed surface. The plan location of these blocks was as shown in Figure 5. The remaining two series of measurements, termed AS1-0B and AS2-7B, are auxiliary runs, carried out for the purposes of comparison and discussion. In the series AS1-0B no blocks were attached to the walls; in the series AS2-7B, four blocks were attached to the right wall and three to the left, in an anti-symmetrical arrangement as shown in Figure 5, the distance between consecutive blocks along each wall being 6m $(= 6B)$. Note that the M or A appearing as the first letter in the name of the measurement series stands for main and auxiliary, S stands for series, and 0B, 2B and 7B indicate the total number of blocks used in the channel. The rationale for the plan arrangement of the blocks is justified in view of the content of Section 4(iv).

In all three series of measurements, 2 minute-long records of instantaneous flow velocity were collected at cross-sections 3 to 20 (Figure 5), and in each cross-section at 17 different points (henceforth referred to as stations). The stations were equally spaced along each cross-section, with stations 1 and 17 located 10cm from the channel walls. The flow velocity oscillograms and plots of time-averaged flow velocity presented later are based on these records. Additionally, 20 minute-long records of instantaneous flow velocity were collected at several stations on cross-sections 6, 12 and 18. These were used to determine the autocorrelation function.

All velocity measurements were carried out at 1cm below the free surface, with the aid of a 2-D Sontek Micro ADV, operating at a sampling frequency of 20 Hz.

4. RESULTS OF MEASUREMENTS

i) As is well-known, by averaging the oscillogram of the time-variation (due to turbulence) of flow velocity over consecutive time-intervals Δt (as done e.g. by Yokosi 1967, etc.), then the "smoothened" oscillograms contain only those velocity fluctuations whose period is larger than Δt. Thus, by selecting a sufficiently large Δt, it is possible to reveal those longest periods (or lowest frequencies) of the velocity fluctuations which are due to the largest structures in the flow, i.e. to reveal the burst-period.

Considering this, the horizontal burst period T_H was determined in this work with the aid of the oscillograms of the longitudinal flow velocity collected over 2 minute-long periods of time. For this purpose, the entire set of available oscillograms (see Section 3) was used. The procedure is illustrated in Figure 6 for the case of the oscillogram corresponding to series MS-2B, cross-section 12, station 15. Figure 6a shows part of the original (2 min-long) oscillogram of the fluctuating component of longitudinal velocity; Figures 6b and c are its smoothened versions, corresponding to $\Delta t = 2s$ and $\Delta t = 8s$, respectively. In this example, the longest periods were exhibited by the curve corresponding to $\Delta t = 8s$, which is partially shown in Figure 6c. In this figure, the solid line is the smoothened oscillogram, and the dashed line was drawn so as to closely follow the trend of the oscillogram while facilitating the determination of the time between its peaks. From the extended (2 minute-long) version of this diagram, it was estimated that the average distance between peaks of the smoothened curve was $\approx 22s$. This value is to be viewed as a sample of the burst period T_H. By repeating this procedure for the entire set of oscillograms corresponding to the main series of measurements MS-2B, it was found that $\approx 18s \le T_H \le \approx 30s$. Taking into account that $\lambda_H = v \cdot T_H$, this gives $\approx 4m \le \lambda_H \le \approx 7m$, i.e. $\approx 4 \le \lambda_H / B \le \approx 7$.

It should be pointed out here that the longest periods of the velocity fluctuations detected in this work can only be due to horizontal turbulence. Indeed, the burst length of the largest vertical structures λ_V is known to be of the order of $\approx 6h$ (see e.g. Jackson 1976, Yalin 1992, Roy et al. 2004). Thus, in the present flow, they are associated with periods of only $\approx 1s$.

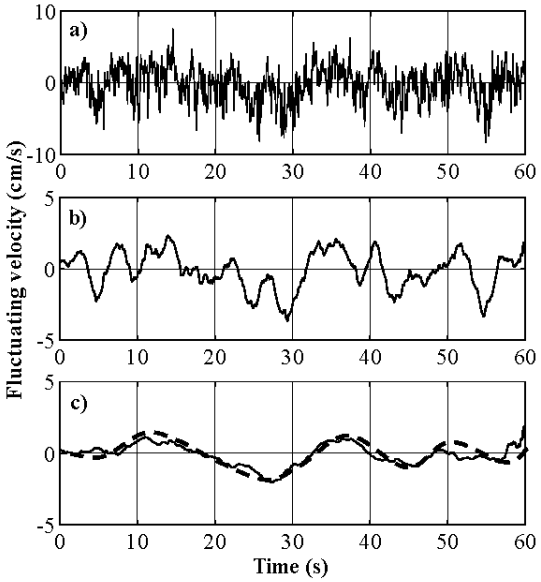

Figure 6. Oscillograms of longitudinal flow velocity, series MS-2B, section 12, station 15. (a) Original data; (b) Averaged over 2s; (c) Averaged over 8s.

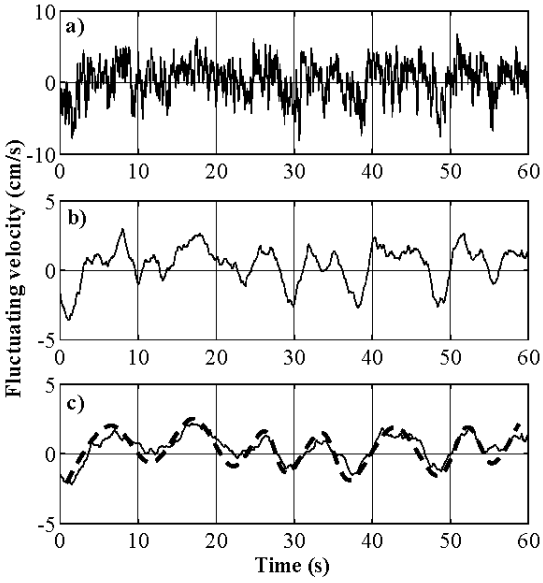

Figure 7. Oscillograms of longitudinal flow velocity, series AS1-0B, section 5, station 6. (a) Original data; (b) Averaged over 2s; (c) Averaged over 4s.

ii) The aforementioned range of values of T_H, and consequently of λ_H, is consistent with that obtained from the plots of the temporal autocorrelation function $R_u(\tau)$ of the longitudinal flow velocities, produced on the basis of the 20-minute long records of velocity mentioned in Section 3. As example, the plot of the temporal autocorrelation function $R_u(\tau)$ corresponding to the record of longitudinal flow velocity at section 18, station 9, series MS-2B, is shown in Figure 8a. Observe from this figure that the velocities separated from each other by the even multiples of $\approx 15s$ are correlated by a positive coefficient of correlation, while those separated from each other by odd multiples of $\approx 15s$ are correlated by a negative coefficient of correlation. Thus, for the particular example in Figure 8a, the "correlation wavelength", to be interpreted as the burst period, is $\approx 30s$.

iii) The range of values of λ_H / B for the series AS2-7B, namely $\approx 4 \le \lambda_H / B \le \approx 7$, is identical to that obtained for the main series MS-2B. However, for the series AS1-0B (where no blocks were attached to the walls), the range of values of T_H was $\approx 9s \le T_H \le \approx 18s$, which implies that $\approx 2 \le \lambda_H / B \le \approx 4$. This is illustrated by Figures 7 and 8b, showing

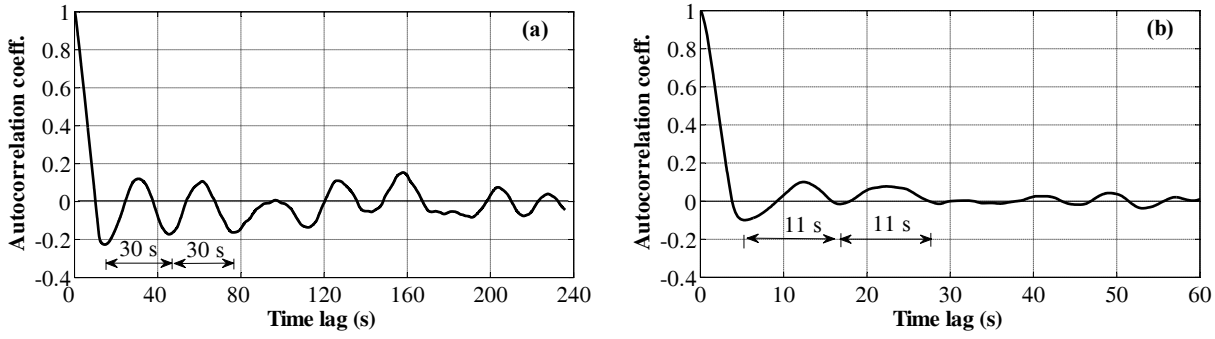

Figure 8. Temporal autocorrelation function of longitudinal flow velocity. (a) Series MS-2B, section 18, station 9, averaging time of 12s; (b) Series AS1-0B, section 6, station 9, averaging time of 4s.

examples of the corresponding flow oscillograms and plots of the temporal autocorrelation function, respectively. Since there is a trend in this series of measurements for the "burst period", and consequently, the "burst length", to increase from the upstream end of the channel to its middle reaches, it is hypothesized here that this is the result of an entrance effect, which, in the absence of the blocks on the walls, is able to "stretch" itself further along the channel.

iv) From the content of this paper, it follows that in the presence of a discontinuity, the straight time-averaged initial flow is subjected to a perpetual action of bursts "fired" from the (ideally speaking) same location (the discontinuity at $x = 0$). This action must inevitably render the flow to acquire a sequence of periodic (along x and t) non-uniformities. Consequently, the time-averaged streamlines – averaged over a multitude of burst periods – must vary along x only (with a period equal to the burst length). These wave-like streamlines deform, in turn, the bed so as to produce the sequence of bed forms whose wavelength is the same as the burst length.

Consider now the case of HCS's and alternate bars. If alternate bars are the "imprints" of HCS's on the bed, and since alternate bars are anti-symmetrical with respect to the x-axis, so must be the sequences of horizontal bursts issued from the right and left banks, respectively. The anti-symmetrical arrangement of the sequences of bursts is shown in Figure 9a. On the basis of the previous paragraph, such burst-sequences should lead to the emergence of wave-like streamlines (Figure 9b). Clearly, for the present case these should appear as an internal meandering of the flow, the action of which on the bed would result in the emergence of alternate bars (Figure 9c).

Considering the aforementioned, cross-sectional plots of local time-averaged longitudinal flow velocity $\overline{u}$ were produced for all cross-sections and all three series of measurements. As example, the resulting plots for cross-sections 9 to 15 corresponding to the series AS2-7B are shown in Figure 10. Here, for the sake of facilitating the drawing, $\overline{u} - \hat{v}$ (where $\hat{v}$ is the average flow velocity at the measurement level) is plotted instead of $\overline{u}$; each dashed horizontal line representing a cross-section is, at the same time, the 'zero' of $\overline{u} - \hat{v}$. These plots are shown together with the plot of the average flow velocity (at the measurement level) for both left and right halves of the channel versus distance along the channel. Observe from the cross-sectional plots of $\overline{u} - \hat{v}$ how the local time-averaged flow velocity goes from being consistently larger towards the left bank from sections 9 to 12, to a nearly uniform distribution at cross-section 13, and then to becoming larger towards the right

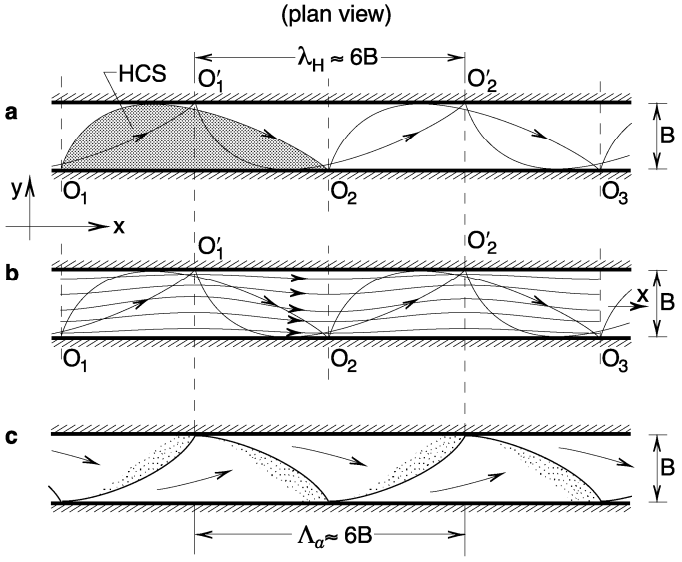

Figure 9. Superimposition of sequence of bursts on the main flow and its consequences

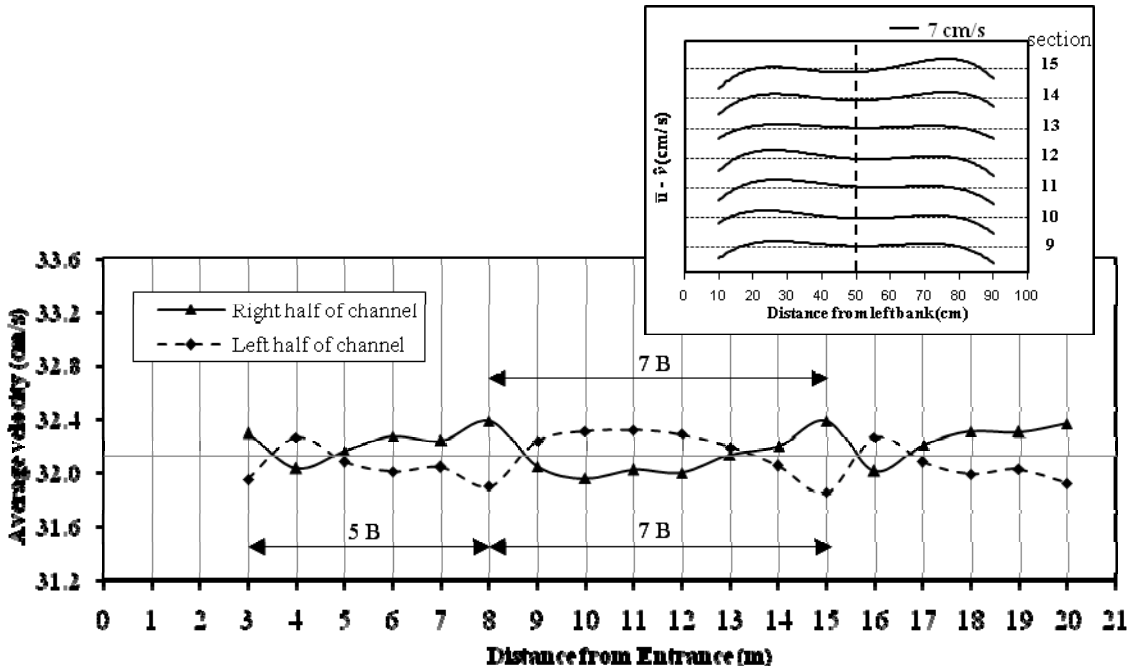

Figure 10. Plots of $\overline{u} - \hat{v}$ at sections 9 to 15 and plot of average flow velocity (at the measurement level) for the left and right halves of the channel for series AS2-7B

bank at sections 14 and 15. The shift of the locus of larger time-average flow velocity from one side of the channel to the other was observed throughout the entire length of the channel, as can be inferred from the plot of the average flow velocity in the left and right halves of the channel. The pattern of plan distribution of $\overline{u}$ implied by the plots in Figure 10 is consistent with the wave-like deformation of the streamlines (the internal meandering) in the schematic Figure 9b. Moreover, the period of this wave-like deformation is generally in agreement with the observed burst length. Although given the paper length limitations, only the plots corresponding to series AS2-7B are shown here, the trends described above were observed also in the other two series of measurements.

5. CONCLUDING REMARKS

The two main findings of this work can be summarized as follows:

1. The horizontal burst length was determined to be between four to seven times the flow width. This value is congruent with the length of alternate bars.
2. A wave-like deformation (internal meandering) of the streamlines was detectable. This is consistent with the existence of periodic sequences of horizontal bursts being "fired" from both left and right walls. It is believed that alternate bars occur through the action on the bed of this deformation, and/or also by the direct action of HCS's on the bed.

The above findings lend support to the view that alternate bars are the "imprints" on the mobile bed of horizontal coherent structures.

ACKNOWLEDGMENTS

This research was supported by funds from the National Science and Engineering Research Council of Canada and the Ontario Research and Development Challenge Fund.

REFERENCES

Blackwelder, R.F. (1978), The bursting process in turbulent boundary layers, *Lehigh Workshop an Coherent Structures in Turbulent Boundary Layers*.

Cantwell, B.J. (1981), Organised motion in turbulent flow, *Ann. Rev. Fluid Mech., Vol. 13*.

da Silva, A.M.F. and El-Tahawy, T. (2008), On the location in flow plan of erosion-deposition zones in sine-generated meandering streams, *J. Hydr. Res.*, Vol. 46, Extra Issue 1, pp. 49-60.

da Silva, A.M.F. (1991), Alternate bars and related alluvial processes, *M.Sc. Thesis*, Queen's University, Kingston, Canada.

Dementiev, M.A. (1962), Investigation of flow velocity fluctuations and their influences on the flow rate of mountainous rivers, *Tech. Report State Hydro-Geological Inst.* (GGI), Vol. 98.

Gad-el-Hak, M. and Hussain, A.K.M.F. (1986), Coherent structures in a turbulent boundary layer, *Phys. Fluids*, Vol. 29, July.

Grishanin, K.V. (1979), Dynamics of alluvial streams, (In Russian) Gidrometeoizdat, Leningrad.

Hayashi, T. (1971), Study on the cause of meanders, *Trans. JSCE*, Vol. 2, Part 2.

Hussain, A.K.M.F. (1983), Coherent structures – reality and myth, *Phys. Fluids*, Vol. 26, Oct.

Jackson, G. (1976), Sedimentological and fluid-dynamic implications of the turbulent bursting phenomenon in geophysical flows, *J. Fluid Mech.*, Vol. 77, pp. 531-560.

Jaeggi, M. (1984), Formation and effects of alternate bars, *J. Hydr. Engrg.*, ASCE, 110(2), pp. 142-156.

Jirka, G.H. and Uijttewaal, W.S.J. eds. (2004), Shallow flows: selected papers of the Int. Symposium on Shallow Flows, 16-18 June 2003, Delft, The Netherlands, A.A. Balkema, Rotterdam, The Netherlands.

JSCE Task Committee on the Bed Configuration and Hydraulic Resistance of Alluvial Streams (1973), The bed configuration and roughness of alluvial streams, *Proc. JSCE*, No. 210, Feb. (In Japanese).

Kamphuis, J.W. (1974), Determination of sand roughness for fixed beds, *J. Hydraul. Res.*, 12(2), pp. 193-203.

Kishi, T. (1980), Bed forms and hydraulic relations for alluvial streams, in *Application of Stochastic Processes in Sediment Transport*, edited by H.W. Shen and K. Kikkawa, Water Resources Publications, Litleton, Colo., Chapter 5.

Klaven A.B. (1966), Investigation of structure of turbulent streams, *Tech. Report State Hydro-Geological Inst.* (GGI), Vol. 136.

Nezu, I. and Nakagawa, H. (1993), Turbulence in open-channel flows, *IAHR Monograph*, A.A. Balkema, Rotterdam, The Netherlands.

Rashidi, M. and Banerjee, S. (1988), Turbulence structures in free-surface channel flows, *Phys. Fluids*, Vol. 31, Sept.

Roy, A.G., Buffin-Bélanger, T., Lamarre, H. and Kirkbride, A.D. (2004), Size, shape and dynamics of large-scale turbulent flow structures in a gravel-bed river, *J. Fluid Mech.*, Vol. 500, pp. 1-27.

Tison, L.J. (1949), Origine des ondes de sable et des bancs de sable sous l'action des courants, *Report II-13*, *3rd Congress IAHR*, Grenoble, France.

Yalin, M.S. (2006), Large-scale turbulence and river morphology, *Proc. River Flow 2006*, 3rd International Conference on Fluvial Hydraulics, Lisbon, Sept. 6-8, Ferreira, Alves, Leal & Cardoso (eds.), Taylor & Francis Group, London, pp. 1243-1249.

Yalin, M.S. and da Silva, A.M.F. (2001), Fluvial Processes, *IAHR Monograph*, IAHR, Delft, The Netherlands.

Yalin, M.S. (1992), River mechanics, *Pergamon Press*, Oxford.

Yokosi, S. (1967), The structure of river turbulence, *Bull. Disaster Prevention Res. Inst.*, Kyoto Univ., Vol. 17, Part 2, No. 121, Oct.